Electric Aircraft Battery Performance: Examining Full Discharge Under Two Conditions

Denner Cunha[1], Brooke Wheeler[2]*, Isaac Silver[3], Gaspar Andre[4]

[1] *Florida Institute of Technology: Melbourne, Florida, US*
   dcunha2022@my.fit.edu - 0000-0002-4366-2966

[2] *Florida Institute of Technology: Melbourne, Florida, US*
   bwheeler@fit.edu - 0000-0001-5507-729X

[3] *Energy Management Aerospace: Satellite Beach, Florida, US*
   isaac@energymanagementaero.com - 0000-0003-0042-7605

[4] *Florida Institute of Technology: Melbourne, Florida, US*
   gandre2020@my.fit.edu - 0000-0002-1786-2139

Abstract

The understanding of battery performance, particularly over the full course of discharge and over battery life is critical to allow pilots to maintain safety in electric aviation. In this study, an electric aircraft powered by two Lithium-Ion battery packs is used as a test article. The objectives of the current study are to build on previous work by conducting two full tests discharging both battery packs from a 100% charge. This allows examination of the battery performance a) under a constant power output and b) with periodic tests of the maximum power available. In addition to state of charge (SOC), remaining flight time, battery temperature, and motor power, this study presents data on motor RPM, torque, voltage, current, battery internal resistance, and available energy. The data on motor power indicates that the available maximum power decreases with lower SOCs when the throttle settings are varied; however, at lower power settings, such as an optimum cruise at 27 kW, the motor power remains constant and as expected during discharge. Also, the constant power setting illustrates that there are inflection points in physical battery characteristics. These results confirm that electric aircraft performance changes during a flight are different than what a pilot expects from a gasoline-powered aircraft. The longer the aircraft flies at different throttle settings, the faster the batteries discharge; the discharge curve is nonlinear. Thus, a piston-trained pilot's expectation for an aircraft's performance later in a flight will not match an electric aircraft.

Keywords

Time Scale of Article

1. Introduction

As aviation moves towards sustainability, one of the technological advances already available is electric aircraft, which are propelled by battery-powered electric motors. When paired with sustainable energy sources, such as solar power, electric aircraft would have the potential to drastically reduce both carbon dioxide emissions as well as other by-products of combustion (Neuman, 2016). An added benefit of fully electric aircraft is a substantial reduction in noise pollution.

Lithium-ion batteries (LIBs) are the dominant chemistry used commercially, although other technologies are being studied to improve aviation battery options (Dornbusch et al., 2022). The energy typically stored in batteries has not reached the ideal density of approximately 500 Wh/kg; instead, 150 to 250 Wh/kg is more commonly available (Tom et al., 2021). Battery development for electric aircraft is ongoing with goals of efficiency, improved range, and performance.

Furthermore, LIBs have exact operational requirements to maintain both performance and battery life including battery temperature maxima and minima and safe voltages (Li et al., 2022). According to recent studies (e.g., Hashem et al., 2020, Tariq et al., 2018), a Battery Management System (BMS) entails monitoring the battery's performance through key indicators such as state of health (SOH), remaining useful life (RUL), and state of charge (SOC).

Essentially, the SOH is meant to assess the aging degree of LIBs, resulting from the difference between the available energy that a battery can currently deliver and its capacity at the beginning of its operational life. According to (Li et al., 2022), a SOH analysis focuses primarily on three health indicators, namely fade capacity, internal resistance, and voltage, enabling an estimation and monitoring of the battery's behavior and age. The RUL, in turn, is predicted as the remaining operational time for a battery before it is decommissioned. Parameters such as lithium concentration available to generate the electrical charge, kinetic energy within the cell, and charge transfer are often used to predict the RUL (Elmahallawy et al., 2022).

The European Aviation Safety Agency (EASA) already has certified electric aircraft in operation. A minimum flight time reserve of 10 minutes in battery charge is required for operations at one airport under EASA regulations (EASA, 2022). Electric aircraft are also operated as experimental aircraft and are likely to be certified by other aviation organizations in the future. This shift in aviation towards electric propulsion requires research on battery management and performance.

As flight time for an electric vehicle is predicated on the ability of the battery to provide the observed power required, this study looked at the max power available at a given SOC as well as the behavior of the battery during a continuous discharge to a low SOC.

The SOC in Battery Management

The SOC is a popular metric for estimating how much electrical energy is still present in a battery. It is defined as the percentage ratio between the available charge at any given time and the total battery capacity (Rozas, et al., 2021). According to (Xu et al., 2020), the estimation of SOC is intended to accomplish a twofold battery performance goal. Firstly, SOC indicates the remaining amount of energy a battery has when compared with the energy it had when fully charged. Secondly, SOC provides the operator with an estimation of how long a battery will last before needing to be recharged. The accuracy of SOC estimation is of crucial importance to the operational safety of a battery pack (Xu et al., 2021).

One of the battery management issues is to determine the lowest SOC below which a battery cannot be safely operated. In their study, (Isikveren et al., 2017) contended that given the fact that a battery is an electrochemical structure, it should not be operated below 20% of its SOC to avoid damage to the electrodes, affecting thereby the battery's operational life.

Testing Battery Characteristics During Discharge

An initial exploration of the battery characteristics during discharge was previously conducted. The SOC, battery temperature, and available motor power were monitored after a regular test flight in an electric aircraft, discharging the batteries from the remaining 53% charge. Battery cell temperatures increased over the course of the test run (maximum 39°C); however, the temperature management was sufficient until a low state of charge. The output for SOC and remaining flight time decreased concurrently, with the exceptions of the first few minutes of the test and very low SOCs. The decrease in maximum available engine power in the last 30% of battery SOC was concerning because it suggested that the expected power may not be available at lower battery SOC, which is when an emergency go-around might be needed.

We wanted to replicate the initial discharge test under controlled conditions. The objectives of the current study were to build on a previous study by conducting two full tests discharging both battery packs from a full (100%) charge. This allowed examination of the battery performance a) under a constant power output and b) with periodic tests of the maximum power available. In addition to SOC, remaining flight time, battery temperature, and motor power, this study presents data on motor RPM, torque, voltage, current, battery internal resistance, and available energy. Furthering our understanding of battery performance, particularly over the full course of discharge and over battery life, is critical to allow pilots to interpret this information during aeronautical decision-making and thus to maintaining safety in electric aviation.

2. Method

The test article was a single-engine electric aircraft powered by two liquid-cooled battery packs. The battery

packs were comprised of cylindrical Lithium Ion cells, with a hybrid matrix of NiMgCo (Nickel Manganese Cobalt). Power is produced by an AC axial-flux motor, which drives a three-blade fixed-pitch propeller mounted directly on the rotor. At full charge (100%), the motor can generate a peak power of 69 kW. The powertrain system also includes an inverter (a.k.a. motor controller), which adjusts the current from the batteries and converts DC to three-phase AC. The test article is certified in Europe by EASA as a light-sport aeroplane (LSA), but not certified in the US, where it operates as an experimental aircraft for research and development purposes.

Because of mandated fuel/power reserves and safety, electric aircraft battery performance cannot be tested to 0% during flight. However, the engine can be run until the batteries fully discharge on the ramp. To execute the experimental runs, the aircraft was tied down by the main landing gear, and the wings were detached from the fuselage.

Two test cases were performed, both starting at 100% battery SOC and completed when 0% was achieved. In Test Case 1, Maximum Take Off Power (MTOP) was initiated, and the throttle setting was gradually reduced to idle. Next, starting when SOC was approximately 75%, for every 10% decrease in battery SOC, the throttle setting was increased to full. In Test Case 2, a constant motor power of 27 kW was maintained during the discharge. This value represents an optimum cruise setting at level flight or a typical cruise power with two passengers onboard, according to the test pilot's experience.

All data output from the aircraft was collected through a flight data recorder at a frequency of 5 Hz. Table 1 summarizes the parameters and units used for the data analysis.

Table 1. Parameters provided by the flight data recorder that were used for the data analysis

Parameter	Unit
Motor Power	kW
Motor RPM	Rpm
Requested Torque	% max. torque
Motor Temperature	°C
Current (Battery Packs 1 & 2)	A
Voltage (Battery Packs 1 & 2)	V
Available Energy (Battery Packs 1 & 2)	kWh
SOC (Battery Packs 1 & 2)	%
SOH (Battery Packs 1 & 2)	%
Average Cells Temp. (Battery Packs 1 & 2)	°C
Remaining Flight Time	min
Elapsed Time	ms

Additionally, other parameters were calculated from the flight recorder data output. In physics, power is the rate at which a force does work and was calculated according to Eq 1 (Tipler and Mosca, 2008).

$$P = F * v \tag{1}$$

P   : power (W)

F   : force acting on the particle (N)

v   : instantaneous velocity (m/s)

Since electric motors involve a rotating shaft, as in a reciprocating engine, power can be related to the rotational properties of torque and angular speed (Eq 2).

$$P = \tau * \omega \therefore P_{Motor} = Q_{Motor} * RPM * \frac{2\pi}{60} \tag{2}$$

τ : torque acting on the particle (N.m)

ω : instantaneous angular velocity (rad/s)

P_{Motor} : motor power (W)

Q_{Motor} : motor torque output (N.m)

RPM   : motor revolutions per minute (rpm)

Electric power is the rate at which electrical energy is transferred by an electric circuit. For a resistor in a DC circuit, the power was calculated by Eq 3 (Tipler and Mosca, 2008).

$$P_{Bat} = V_{Bat} * I_{Sys} \tag{3}$$

P_{Bat} : power available from the battery pack (W)

V_{Bat} : battery pack voltage (V)

I_{Sys} : current required by the motor-controller (A)

Finally, battery internal resistance was calculated using Eq 4.

$$R_{Bat} = \frac{V_{Bat}}{I_{Sys}} \tag{4}$$

R_{Bat} : battery internal resistance (Ω)

3. Results and Discussion

Regular flight tests have indicated battery SOC and motor performance decreasing as expected during the battery discharge. These findings confirmed the initial test run previously conducted for the last 53% SOC. This experiment used two different throttle settings to fully discharge the batteries from 100% SOC to 0%; the battery packs were at a SOH of 88% for this study. The discharge was accomplished in approximately 53 minutes in both test cases.

The basic battery characteristics data are presented in Table 2 for Test Case 1 and Table 3 for Test Case 2. These results will be discussed and analyzed throughout this section, along with additional data.

Fig. 1 shows the motor power over the course of the battery's discharge. In Test Case 1, the throttle was advanced to full and was gradually reduced to idle. Next, when SOC was approximately 75%, full throttle was set

at approximately every 10% decrease in the battery SOC. In Test Case 2, the pilot kept a constant cruise power setting of 27 kW

**Table 2.** Test case 1: data for MTOP and test of maximum power after each 10% decrease in SOC.

SOC [%]	Motor Power [kW]	Motor RPM [rpm]	Voltage per battery pack [V]	Current per battery pack [A]
100	67	2377	399	93.4
75	65	2325	348	93.5
70	64	2294	343	93.8
60	63	2330	333	96.3
50	63	2343	323	98.9
40	62	2309	315	99.8
30	62	2282	311	101.9
22	61	2226	305	101.5
15	53	2162	301	90.2
10	57	2232	294	101.7

Note that in Test Case 1, while the full engine power of approximately 65 kW was achievable for most of the test, as the SOC of the battery decreased, so did the maximum motor power. After battery SOC dropped to 45%, the reduction in maximum power was above 10%. Below 15%

SOC, the power generation became unpredictable, and the maximum power was substantially lower than that listed for the motor. Thus, at lower SOCs, the motor does not produce the maximum rated power at a full throttle setting. At a SOC of approximately 6%, the batteries lost the ability to supply power, even though 0% SOC had not been achieved yet.

Table 3. Test case 2: data for constant 27 kW power discharge.

SOC [%]	Motor Power [kW]	Motor RPM [rpm]	Voltage per battery pack [V]	Current per battery pack [A]
100	27	1800	385	37.4
75	27	1800	360	39.1
70	27	1800	356	39.6
60	27	1800	348	40.5
50	27	1800	339	41.6
40	27	1800	331	42.5
30	27	1800	323	44
22	27	1800	318	44.4
15	27	1800	313	45.1
10	27	1800	309	45.8
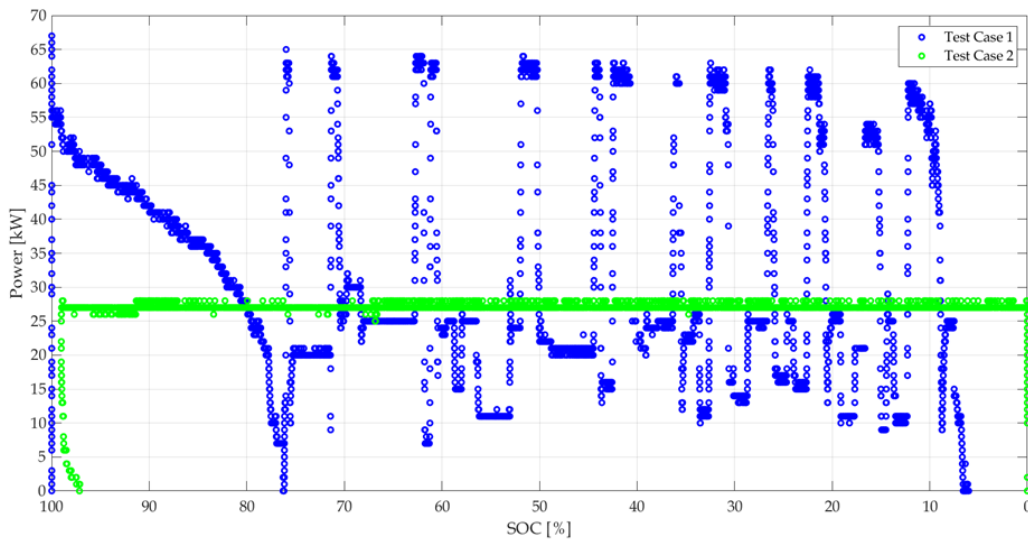
Fig. 1. Motor Power over the course of the battery's discharge

The pilot advanced the throttle to full at approximately 10% SOC intervals. Full throttle could not be continuously maintained because of the motor high temperature limits. The battery temperature remained within limits for the test. At no time did the motor or battery exceed the specified maximum temperature limits.

In Test Case 2, on the other hand, the battery's ability to supply power was consistent throughout the discharge. This constant power output was as expected and

indicates that at intermediate power settings the batteries provided the expected power across the entire discharge run.

Through motor power and RPM (Fig. 2), torque output was calculated using Eq 2. Next, the values were normalized and compared with the requested torque extracted from the data logger, as shown in Fig. 3.

As with any mechanical system, electrical motors also present a loss in torque during the conversion of

electrical energy into mechanical energy. Thus, as expected, the data in Fig 3 was concentrated above the red diagonal line, indicating that the torque requested by the motor controller was greater than the torque output produced by the 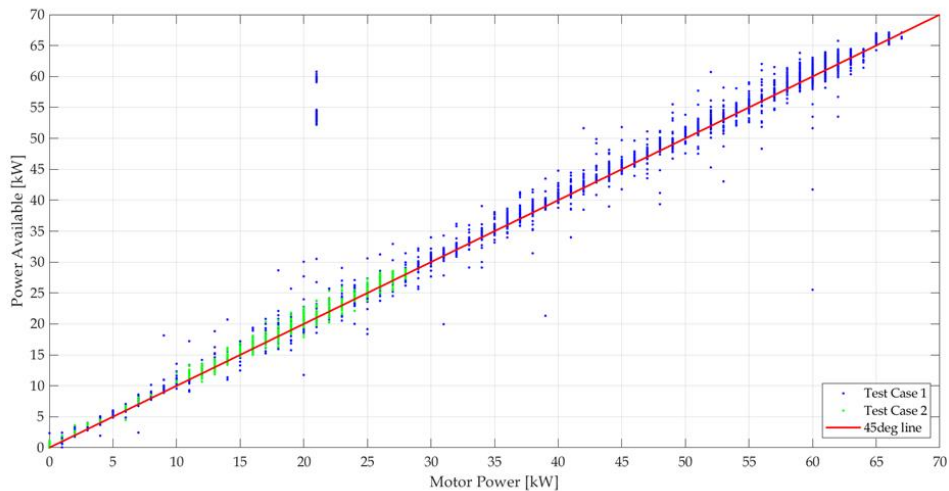motor. The same relationship can be observed between the motor power and the power available (Fig. 4) from the battery pack, which was calculated via Eq 3. After eliminating the outliers, a mean value of approximately 3% in loss of power was found.
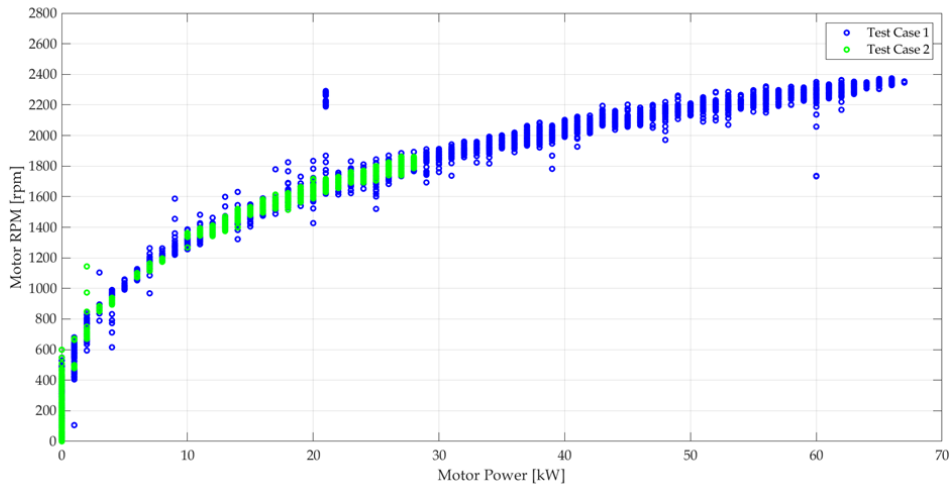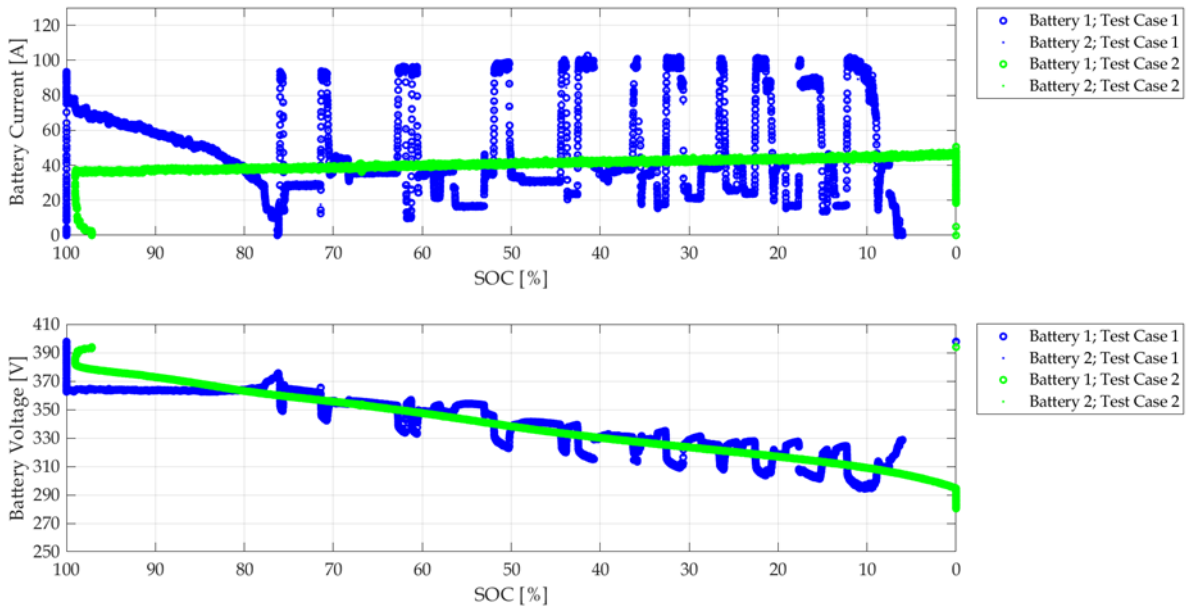

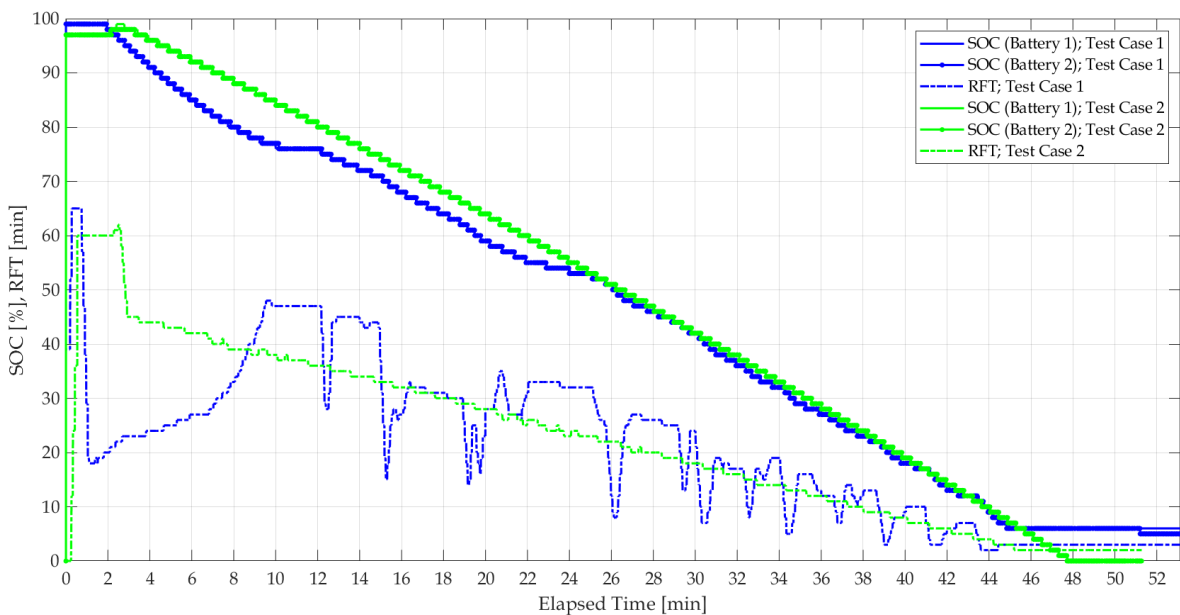**Fig. 2.** Motor RPM vs. Motor Power
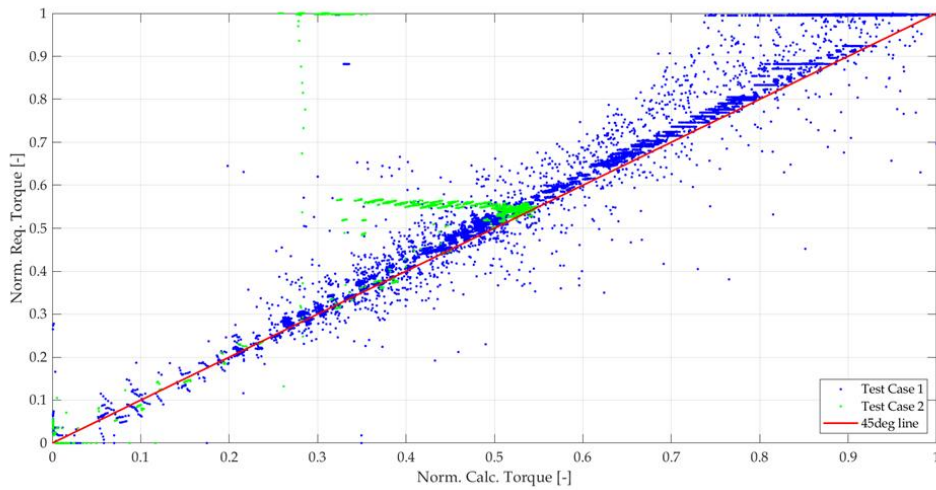
Fig. 3. Normalized Requested Torque vs. Normalized Calculated Torque

Fig. 4. Power Available vs. Motor Power

Fig. 5. Current and voltage provided by the battery packs over the course of the discharge

Fig. 6. State of Charge and Remaining Flight Time

Fig. 5 shows the voltage and current readings obtained during the discharge of the batteries. The data for batteries 1 and 2 are superimposed on each other, indicating their comparable performance. This supports the reliability of the battery packs as both batteries behaved similarly. As can be noted, the voltage of the batteries drops along the discharge curve. Therefore, to deliver power to the motor, the motor controller requires a higher current (see Eq 3). This behavior is evident in Test Case 2 and can be noted by comparing each peak of battery current in Test Case 1 (see Table 2). Note that at higher SOCs (above 45%), when maximum power is requested, the current output is maintained, resulting in a flat peak at the maximum power achieved.

However, as SOC decreases, the current drops off almost immediately, creating a curved decline in current. This is particularly evident at 10% SOC.

Fig. 6 depicts both remaining flight time (RFT) and state of charge (SOC), which is equivalent between both battery packs. Both parameters are plotted on the same scale.

As expected, both curves decrease over the course of the test runs. In Test Case 2, SOC remains quite linear along the discharge due to the constant motor power. However, in both test cases, initial estimates of flight time in the first few minutes are severely low. The RFT estimated during the final seven minutes in Test Case 1

remains constant, as does the SOC, until no battery power is delivered. The dips in the RFT in Test Case 1 occur during the maximum engine power tests. SOC and RFT did not agree at various times, creating a confounding decision-making environment for pilots. In a traditional fuel-burning aircraft, the endurance calculation is a well-known procedure, and it is based on the amount of fuel contained in the tanks. For an electric vehicle, the overall energy available and energy consumption are less trivial to assess, and new metrics never used before may be required to accurately depict the energy state (Verberne et al., 2022).

Both batteries and motor temperatures were monitored until the very end of the test cases. Fig. 7 shows that the motor temperature increased substantially in the first 12 minutes, but then stabilized at approximately 75°C. Both batteries had approximately the same average

temperature. The thermal management system worked well overall, but in the final minutes, the battery temperature increased, reaching 48°C as battery SOC approached 0. This temperature was nine degrees higher than the maximum battery cell temperature (39°C) reached during the previous study; this difference is likely due in part to this study conducting a discharge starting from 100%, and the higher SOH of the batteries during the prior study.

Battery internal resistance depends on the battery age, the battery temperature, and the battery SOC (Favier et al., 2021). This parameter was calculated through Eq 4 and is graphically presented in Fig. 8. Data from Test Case 2 shows that the internal resistance decreases when battery temperature increases. The peaks observed in Test Case 1 are related to the voltage drops when maximum discharge power was required.
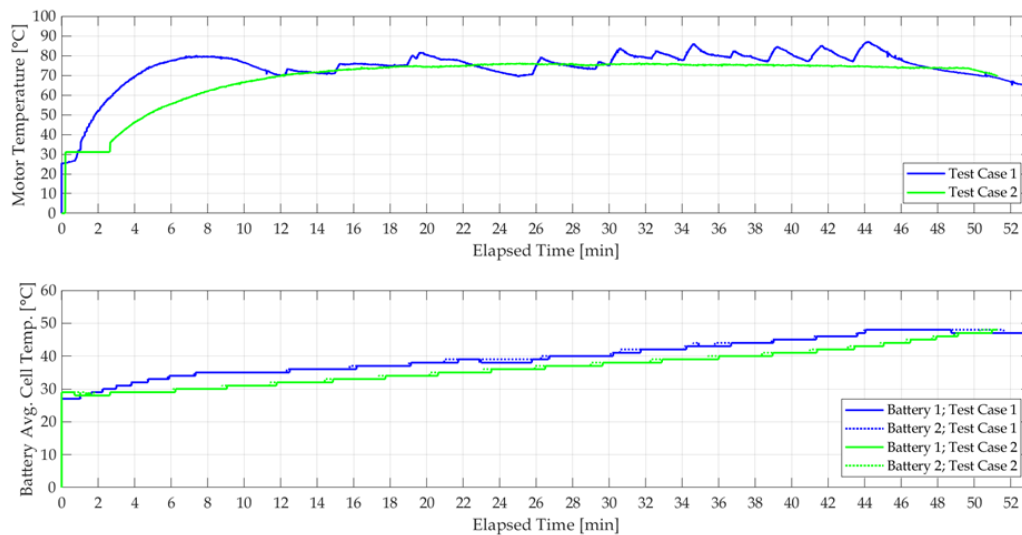
Fig. 7. Motor and Battery Cells Average Temperatures
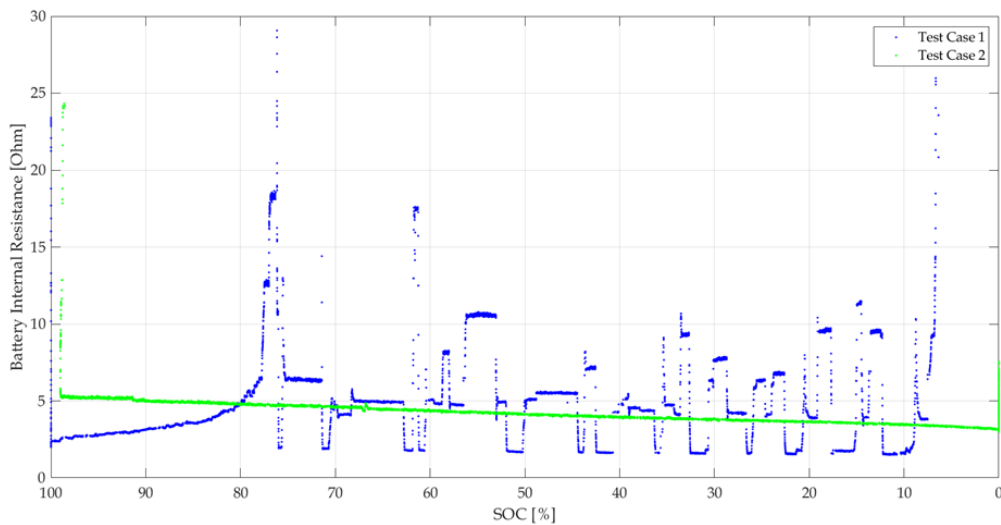
Fig. 8. Battery Internal Resistance varying with temperature, SOC, and voltage drops. Battery Internal Resistance varying with temperature, SOC, and voltage drops
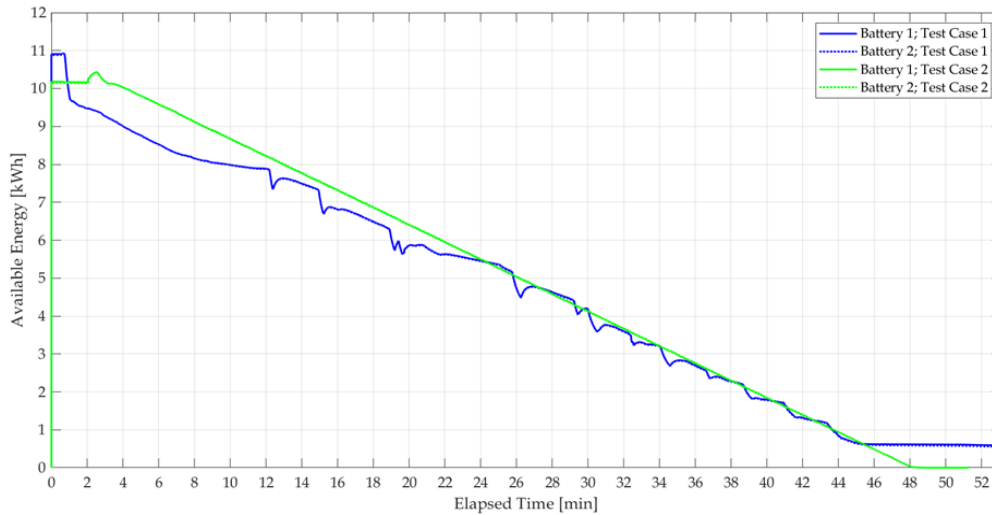
Fig. 9. Available energy for each battery pack over the course of the discharge

Finally, Fig. 9 presents the available energy for each battery pack over the course of the discharge. This parameter indicates the amount of energy that the battery manages to supply the motor controller at a given power setting, considering all losses. Test Case 1 demonstrates that as more power is requested during the discharge cycle, less energy has become available

4. Conclusions

The data on motor power indicates that the available maximum power decreases with lower SOCs when the throttle settings are varied (e.g., Test Case 1); however, at lower power settings, such as an optimum cruise at 27 kW, the motor power remained constant and as expected during discharge. In Test Case 2, the constant power setting illustrated that there are inflection points in physical battery characteristics. As temperature increases and SOC decreases, the voltage also decreases. The changes in battery characteristics are not linear, however. These test runs verified that as SOC decreases below 45% and with higher temperatures, there is more resistance in the batteries.

Pilots cannot continuously interact with the battery information display. This means that an electric aircraft may move into a state of decreased performance with no warning to the pilot. Pilots will need to be aware of lower maximum power availability at low SOCs, especially in the event of an emergency go-around. The study provided invaluable insight into a battery's remaining operational life to aid pilots' decision-making for safer and optimized flight planning with respect to electric aircraft.

For a given aircraft, the battery performance and characteristics should be determined in order to better educate pilots on aircraft performance. One of the advantages of battery-powered aircraft is that as new battery chemistries and/or technologies become available, the batteries in an electric aircraft can be switched out. However, a characterization of the battery performance with the airframe is crucial for understanding performance with what effectively amounts to a new form of fuel.

These results confirm that electric aircraft performance changes during a flight are different than what a pilot expects from a gasoline-powered aircraft. In a piston aircraft, the rated maximum power available at full throttle remains constant throughout the flight, while the weight of the aircraft is decreasing. This results in increased performance near the end of a flight because of the decreased weight due to the burned fuel. However, in the test article, and presumably other battery-powered aircraft, the weight remained constant, and there was lower performance (i.e., motor power) at the lower SOC near the end of the test runs. The longer the aircraft flies at different throttle settings, the more difficult it is for the operator to predict the battery states and, therefore, the usable energy; the discharge curve is nonlinear. Thus, a piston-trained pilot's expectation for an aircraft's performance later in a flight will not match an electric aircraft.

The basic battery characteristics data are presented in Table 2 for Test Case 1 and Table 3 for Test Case 2. These results will be discussed and analyzed throughout this section, along with additional data.

Nomenclature

AC	: Alternate Current
BMS	: Battery Management System
DC	: Direct Current
EASA	: European Aviation Safety Agency

LIBs : Lithium-Ion Batteries

LSA : Light-Sport Aeroplane

MTOP : Maximum Take Off Power

NiMgCo : Nickel Manganese Cobalt

RPM : Revolutions per Minute

RFT : Remaining Flight Time

RUL : Remaining Useful Life

SOC : State of Charge

SOH : State of Health

US : United States

CRediT Author Statement

Denner Cunha: Software, Formal analysis, Data Curation, Visualization, Writing- Original Draft, Writing- Review & Editing. **Brooke Wheeler**: Conceptualization, Coordinated Research Efforts, Resources, Writing- Original Draft, Writing- Review & Editing, Supervision, Project Administration, Funding Acquisition. **Isaac Silver**: Conceptualization, Methodology, Investigation, Resources, Writing- Original Draft, Writing- Review & Editing, Project Administration, Funding Acquisition. **Gaspar Andre**: Writing- Original Draft, Writing- Review & Editing.

References

Dornbusch, D., Viggiano, R. P., Wu, J., Lin, Y., Connell, J., and Lvovich, V., 2022. Design Considerations for Practical Li-S Battery Components for Electric Aviation. ECS Meeting Abstracts, Volume MA2022-01, A01: New Approaches and Advances in Electrochemical Energy Systems. Abstr. MA2022-01 133.

Elmahallawy, M., Elfouly, T., Alouani, A., and Massoud, A. M., 2022. A Comprehensive Review of Lithium-Ion Batteries Modeling, and State of Health and Remaining Useful Lifetime Prediction. IEEE Access, 9(2022), vol. 10, pp. 119040-119070, 2022, doi: 10.1109/ACCESS.2022.3221137.

European Union. Easy Access Rules for Air Operations (Regulation (EU) No 965/2012), ED Decision 2022/005/R, AMC1 NCO.OP.125. Page 1837(2022). https://www.easa.europa.eu/downloads/20342/en.

Favier, A., Roberts, S., Esfeld, J., and Uchida, J., 2021. Things Flight Testers Should Know About Batteries for Electric Propulsion. 52nd SFTE International Symposium. St. Louis, MO, 2021.

Hashem, S. R., Roja, E., Nazari, A., Aliniagerdroudbari, H., Alhadri, M., Zakri, W., Mohammed, A.H., Mahajan, A., and Farhad, S., 2020. A Fast Diagnosis Methodology for Typical Faults of a Lithium-Ion Battery in Electric and Hybrid Electric Aircraft. Journal of Electrochemical Energy Conversion and Storage. 17(2020), 011011-1. https://doi-org.portal.lib.fit.edu/10.1115/1.4044956.

Isikveren, A. T. , Pornet, C., Vratny, P. C., and Schmidt, M., 2017. Optimization of Commercial Aircraft Using Battery-Based Voltaic-Joule/Brayton Propulsion. Journal of Aircraft, vol. 54, p.p. 246-261, 2017, doi: 10.2514/1.C033885, https://doi.org/10.2514/1.C033885.

Li, R., Hong, J., Zhang, H., and Chen, X., 2022. Data-driven battery state of health estimation based on interval capacity for real-world electric vehicles. Energy, vol. 257, 2022, 124771, ISSN 0360-5442, https://doi.org/10.1016/j.energy.2022.124771.

Neuman, T., 2016. Fly the Electric Skies. IEEE Spectrum 53(2016), 6, 44-48.

Rozas, H., Troncoso-Kurtovic, D., Ley, C. P., and Orchard, M. E. (2021). Lithium-ion battery State-of-Latent-Energy (SoLE): A fresh new look to the problem of energy autonomy prognostics in storage systems. Journal of Energy Storage, 40(2021), 102735, https://doi.org/10.1016/j.est.2021.102735.

Tariq, M., Ali, I. Maswood, A. I., Gajanayake, C. J., and Gupta, A. K. (2018). Modeling and Integration of a Lithium-Ion Battery Energy Storage System with the More Electric Aircraft 270 V DC Power Distribution Architecture. IEEE Access, 6(2018), 41785-41802.

Tipler, P. and Mosca, G., 2008. Physics for Scientists and Engineers, 6th ed. W.H. Freeman and Company, New York, NY.

Tom, L., Khowja, M., Vakil, G., and Gerada, C., 2021. Commercial Aircraft Electrification—Current State and Future Scope. Energies. 14(2021), 8381. https://doi.org/10.3390/en14248381.

Verberne, J., Beedie, S., Harris, C., Justin, C., and Mavris, D., 2022. Development of a Simulation Environment to Track Key Metrics to Support Trajectory Energy Management of Electric Aircraft. AIAA Aviation 2022 Forum, 2022. Chicago, Illinois. (Published). https://doi.org/10.2514/6.2022-3255.

Xu, Z., Wang , J., Fan, Q., Lund, P. D., and Hong, J., 2020. Improving the state of charge estimation of reused lithium-ion batteries by abating hysteresis using machine learning technique. Journal of Energy Storage, vol. 32, 2020, 101678, ISSN 2352-152X, https://doi.org/10.1016/j.est.2020.101678.